CHAPTER 5

PHASE CHANGES IN TERNARY NICKEL-BASE ALLOYS

5.1 Introduction

Phase transformations exhibited by selected alloys of two ternary nickel-base systems, nickel-chromium-aluminium and nickel-titanium-aluminium, are examined in the present chapter. These materials approach commercial alloys more nearly in composition and microstructre than the binary alloy of Chapter 4 (see Chapter 1 above). One nickel-chromium-aluminium alloy was chosen to illustrate some behavioural changes associated with the reduction in lattice misfit associated with chromium addition. Two alloys containing nickel, aluminium and titanium were selected as models for second phase production from these three principle components of superalloy γ'.

The present investigation applies to ternary alloy studies the same set of experimental techniques which were employed in examination of Ni-14.1at.%Al (Chapter 4) and changes in partitioning and phase separation behaviour are followed. These studies of more complex systems are extended in Chapter 6 to examination of a six-element model of commercial alloy PE16.

5.2 Nickel-Chromium-Aluminium

5.2.I Microstructure of the nickel-chromium-aluminium system

5.2.I.1 Constitution

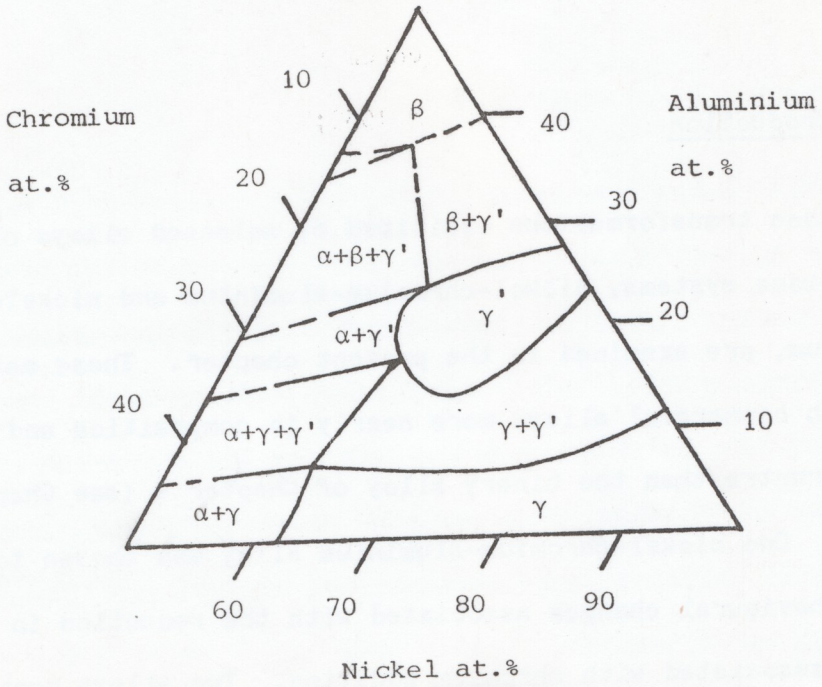

Figure 5.1 The nickel-chromium-aluminium phase diagram: isothermal section for 750°C (after Taylor and Floyd 1952b).

A section of the nickel-chromium-aluminium phase diagram for 750°C (Taylor and Floyd 1952b) is shown in figure 5.1.. The phase field of the γ' phase of nickel-aluminium alloys is considerably increased by the addition of chromium, but there is no equivalent Ni_3Cr phase (Taylor and Hinton 1952; Nordheim and Grant 1953). The γ' precipitate of the ternary alloys is regarded as $(Ni,Cr)_3(Al,Cr)$, in which the nickel and aluminium atoms seek out pure phase sites and chromium is partitioned between the sub-lattices (Dorfeld and Phillips 1970).

Below 590°C the nickel-chromium system does, however, contribute a second phase, orthorhombic D^{25}_{2h}, ordered Ni_2Cr (Baer 1956, 1958; Vintaykin and Urushadze 1969; Taunt and Ralph 1975). Very little appears to be known concerning the effect of this phase upon ternary and general superalloy equilibria as the composition lies well outside those experienced, even locally, in most alloys of interest. However, its presence should be borne in mind in materials of high chromium content and particularly in those which also contain a high volume fraction of γ' because local matrix concentrations of chromium may be raised still further by rejection of the element from the second phase.

5.2.I.2 Morphology and properties

A range of precipitate morphologies may be achieved in nickel-chromium-aluminium alloys by control of lattice mis-match between matrix and γ' phases. In situations of complete coherency (zero mis-match) the second phase precipitates as spheres (Gleiter and Hornbogen 1965a; reviews Gleiter and Hornbogen 1967a; Merrick 1978). With increasing misfit this morphology changes to cuboidal (Gleiter and

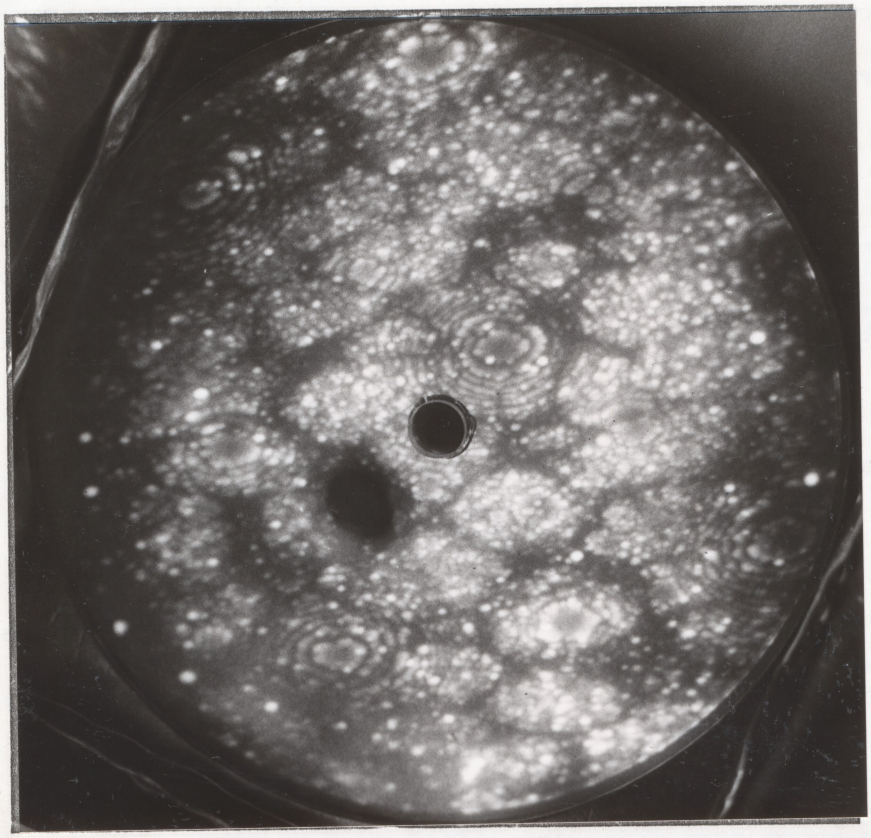

Figure 5.2 Field-ion micrograph of Ni-20.0at.%Cr-14.0at.%Al alloy aged for 5 minutes at 625^{o}C.

Hornbogen 1967a; Gibbons and Hopkins 1971). Observations of dispersed globular γ' have been recorded by Taylor and Floyd 1952b and Chellman and Ardell 1974. A replacement reaction of cellular precipitation has also been noted by Hornbogen and Roth 1967, but this is thought to be related to increasing supersaturation and not to lattice misfit.

Particle distributions are likewise related to lattice misfit: spherical precipitates show homogeneous distribution (Hornbogen and Roth 1967), with no preferred alignment (Tyapkin, Travina and Kozlov 1975). Alloys of greater misfit present aligned microstructures with particle distributions related to the misfit (Chellman and Ardell 1974). All distributions obey a $t^{1/3}$ coarsening law (e.g. Gleiter and Hornbogen 1967a; Rastogi and Ardell 1974), with no correction required for volume fraction of second phase. (Chellman and Ardell 1974).

Strengthening by γ' has been investigated by Gleiter and Hornbogen 1967b; Ham 1970; Hornbogen and Mukherjee 1964).

5.2.II Results

5.2.II.1 Atom-Probe Microscopy

5.2.II.1i Qualitative observations

A two-phase microstructure was present at all stages of ageing, including the as-quenched state. Overall field-ion images indicated that the copious, brightly-imaging second phase was at least partly aligned even from the quench. Figure 5.2 illustrates the alignment after 5 minutes heat treatment at 620°C. Initially, the phase appeared to be globular. After 2 hours ageing cuboidal morphology had developed. At all stages this phase displayed series of alternating

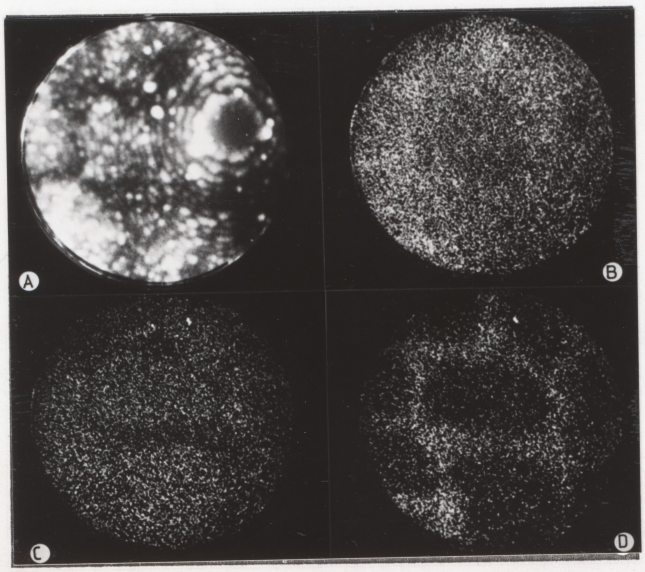

Figure 5.3 IAP images from the specimen shown in figure 5.2.
a) FIM image, b) Ni^{2+}, c) Al^{2+}, d) Cr^{2+}.

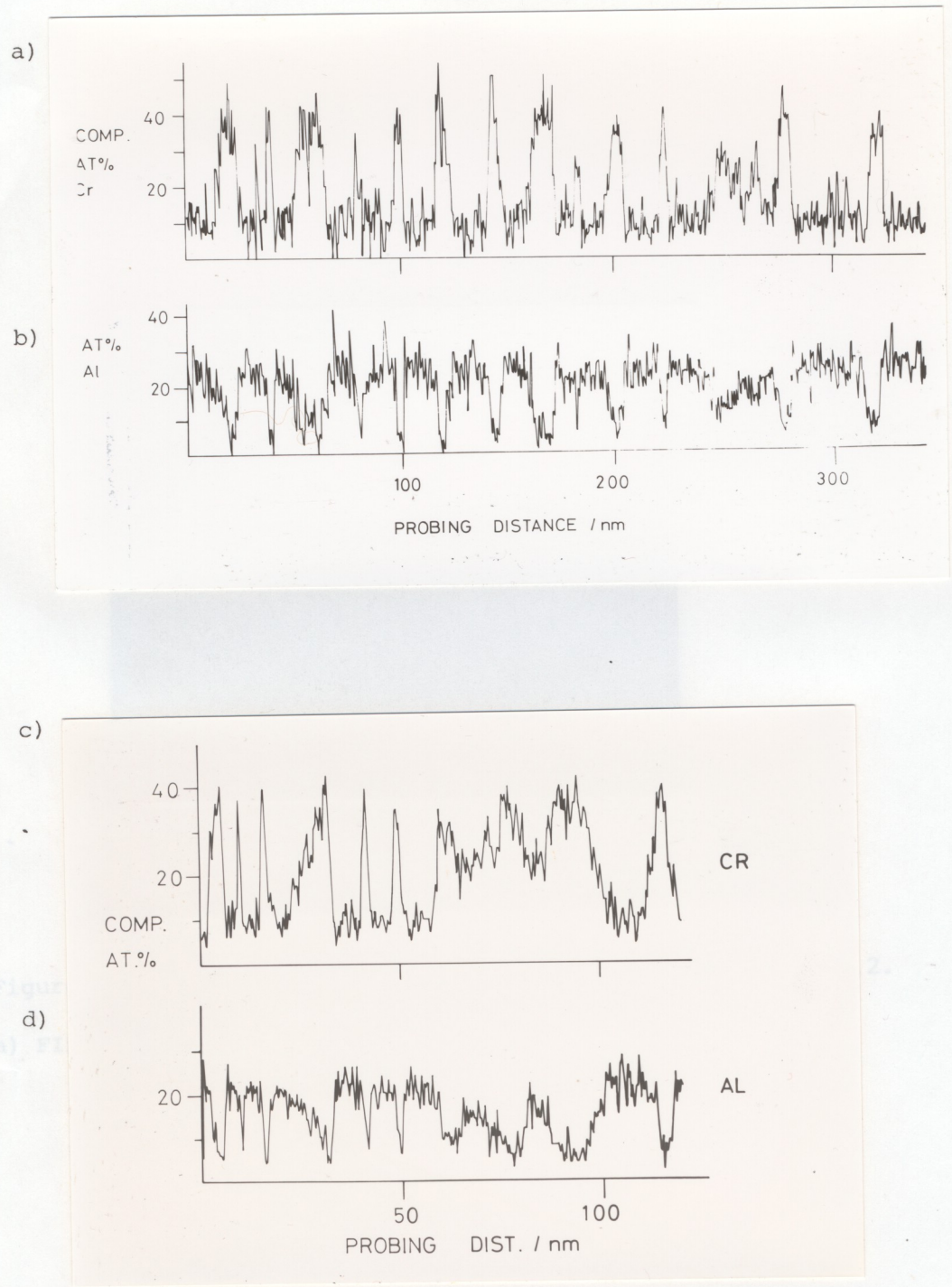

Figure 5.4 Composition profiles from specimens aged for 2 minutes (a and b), and 20 minutes (c and d), at 620°C.

bright and dim rings characteristic of at least partially ordered structures (e.g. Taunt 1973). No regular structure or variations in imaging properties were shown by the remaining phase.

IAP analyses showed that all three alloying elements were present in both phases throughout the ageing sequence. Figure 5.3 presents gated images of Ni^{2+}(b), Al^{2+}(c) and Cr^{2+}(d) from an area (a) of the specimen shown in figure 5.2. It may be seen that the phase of enhanced contrast is aluminium-rich. Nickel and chromium partition preferentially to the remaining regions.

No major changes in elemental partitioning between phases were noted throughout the heat treatment cycle.

5.2.II.1ii Quantitative studies I : general phase analysis

QAP analyses confirmed the presence of all three elements in both phases throughout ageing. Figure 5.4 shows two sets of composition profiles, each set comprising one chromium and one aluminium trace, from specimens aged for 2 minutes (figure 5.4a,b) and 20 minutes (figure 5.4c,d) at 620°C. Within each pair the aluminium and chromium concentrations vary roughly in antiphase.

Detailed QAP analyses of the individual phases were also performed. With the exception of the 2 hour heat treatment 7-14 samples of each phase were taken per heat treatment. Mean compositions, ($\bar{c}$), of the phases at each ageing stage were then derived by summation of appropriate ion counts from samples of similar overall composition. In some cases compositions apparently clustered around more than one mean and separate summations were performed for

Table 5.1 QAP Analyses of Ni -20.0at%Cr-14.0at%Al: Aluminium-Rich Phase

Ageing time @ 620°C/mins.	Al/at%	Cr/at%	Ni/at%
0 (quenched)	23.25 ±0.35	9.40 ±0.22	67.35 ±0.60
2	22.68 ±0.27	9.64 ±0.17	67.19 ±0.46
5	15.19 ±1.60	9.75 ±1.28	75.06 ±3.56
	17.23 ±0.41	9.34 ±0.30	73.42 ±0.86
	25.86 ±0.67	11.02 ±0.44	63.12 ±1.05
20	21.20 ±0.34	9.37 ±0.22	69.43 ±0.61
120	16.91 ±0.97	9.32 ±0.72	73.77 ±2.03
	21.56 ±1.06	8.25 ±0.66	70.20 ±1.91

Table 5.2. QAP Analyses of Ni-20.0at%Cr-14.0at%Al :Chromium-Rich Phase

Ageing time @ 620°C/mins.	Al/at%	Cr/at%	Ni/at%
0 (quenched)	8.82 ±0.70	30.75 ±1.31	60.44 ±1.84
	10.89 ±0.26	31.79 ±0.45	57.32 ±0.60
	12.14 ±0.71	26.38 ±1.05	61.49 ±1.61
2	6.84 ±0.30	36.93 ±0.70	56.24 ±0.86
5	5.70 ±0.21	34.97 ±0.53	59.34 ±0.69
	8.16 ±0.51	27.65 ±0.94	64.19 ±1.43
	13.24 ±0.58	24.64 ±0.79	62.12 ±1.25
20	7.06 ±0.26	34.10 ±0.57	58.85 ±0.75

5.6

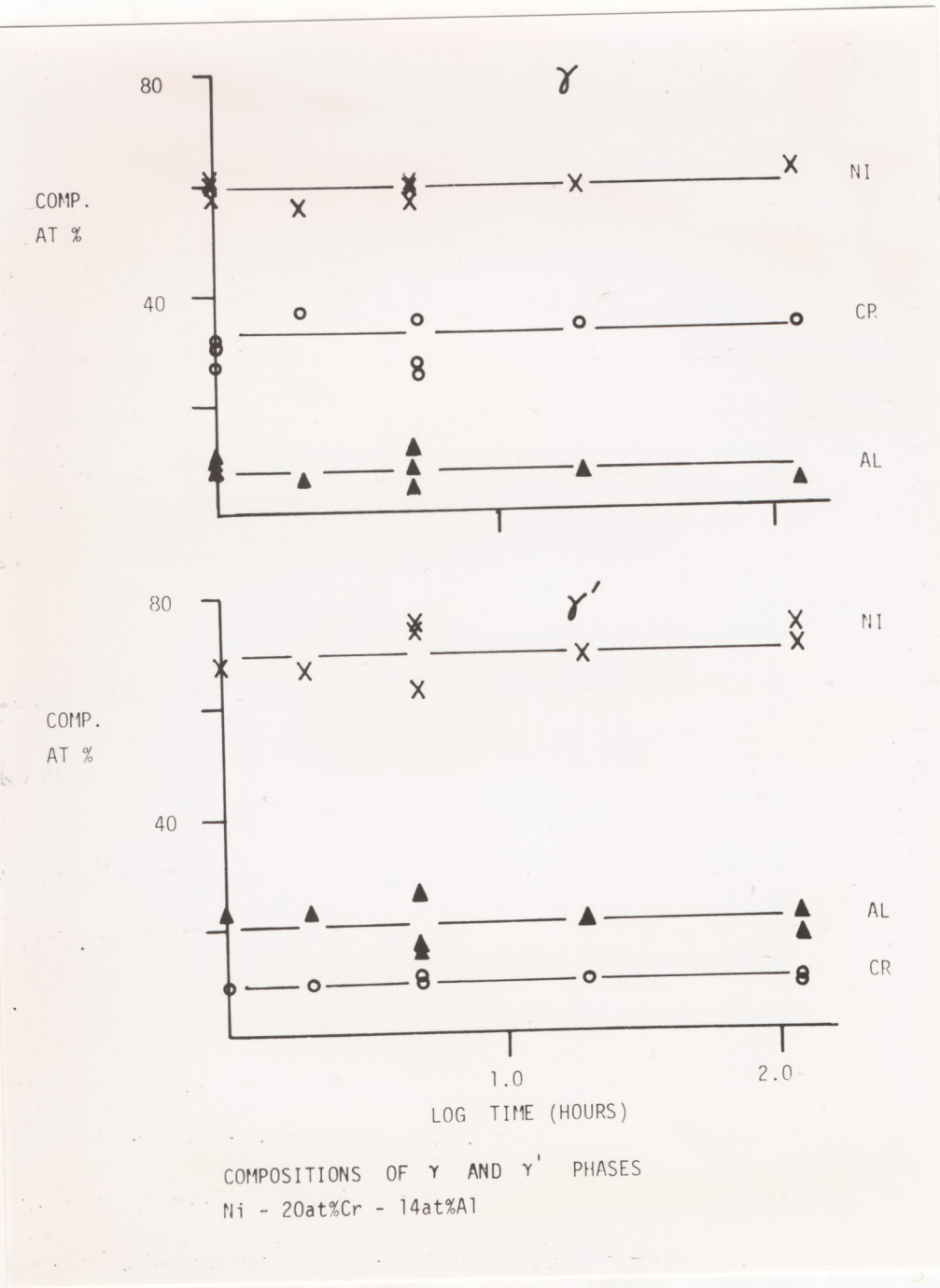

5.5

Figures 5.5 and 5.6 Compositions of aluminium-rich phase (fig. 5.5) and chromium-rich phase (fig. 5.6) as a function of ageing time.

each population. The errors in these determinations were estimated as $(\sqrt{cn}/n)$, where n is the number of ions considered.

The results of these analyses are presented numerically in Tables 5.1 (aluminium-rich phase) and 5.2 (chromium-rich phase) and graphically in figures 5.5 and 5.6 respectively. Figure 5.6 also contains additional small volume analyses for the 2 hour heat treatment.

Overall the data show that phase compositions remain approximately constant during heat treatment. A very small overall decrease in aluminium content was noted after long ageing sequences. This may be attributed to loss of the element from the specimen surface during heat treatment. Approximate mean compositions derived from figures 5.5 and 5.6 were : aluminium-rich phase $Ni_{70.0}{}^{Al}{}_{20.5}{}^{Cr}{}_{9.5}$ and chromium-rich phase $Ni_{59.5}{}^{Cr}{}_{34.0}{}^{Al}{}_{6.5}$.

Treatment of QAP traces as linear samples of microstructure gave volume fractions of aluminium-rich phase in the range 45-65%. No trend in volume fraction was seen with ageing. Given the phase compositions determined above a value of 55volume% would correspond to a net melt composition of Ni-20.0at.%Cr-14.0at.%Al. The range of wet chemical analyses was Ni-16.7at.%Cr-14.5at.%Al to Ni-20.0at.%Cr-14.0at.%Al.

Examined in more detail the various composition measurements (figures 5.5 and 5.6) for both phases after 5 minutes heat treatment and possibly also after 2 hours indicate that two γ' populations are present. For the former ageing time the compositions are approximately Ni-17at.%Al-9at.%Cr and Ni-26at.%Al-11at.%Cr for the

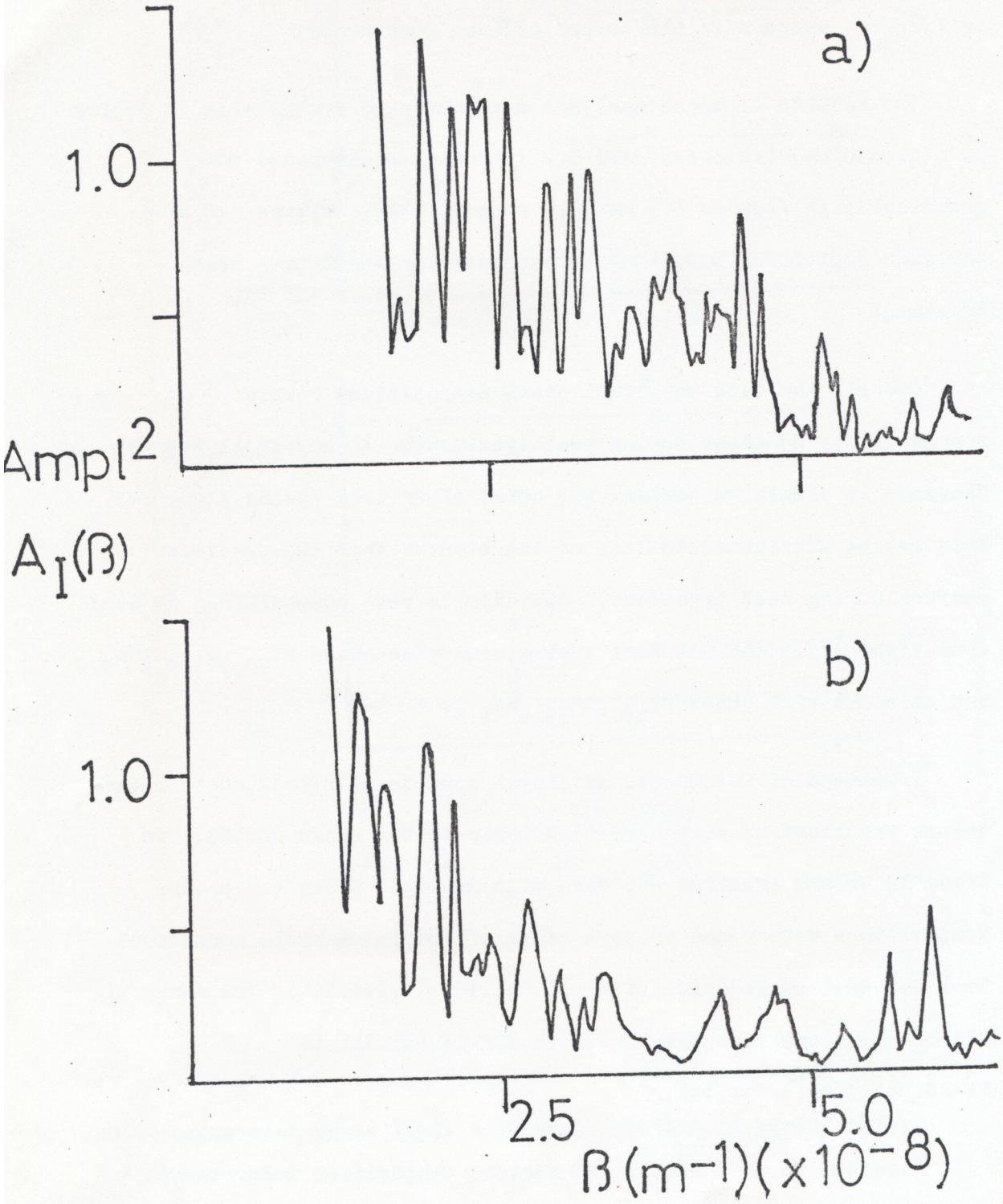

Figure 5.7 Net Fourier transforms for the composition profiles shown in figure 5.4: a)Al-rich phase, b)Cr-rich phase.

aluminium-rich phase. In the chromium-rich phase values are Ni-6at.%Al-35at.%Cr and Ni-13at.%Al-25at.%Cr.

Examination of the original data showed that no particular precipitate population was confined to an individual specimen or to results from a single atom probe. Thus the compositional duality may be assumed to be real.

5.2.II.1iii Quantitative studies II : particle distribution

The technique of Fourier analysis described in Chapter 3 above was applied to QAP profiles in order to test for dominant periodicity. In each case two transforms were made : one of the aluminium trace (assuming a pseudo-binary system nickel/chromium - aluminium (see Morral 1972)) and the second for chromium (pseudo-binary nickel/aluminium - chromium). The results of these analyses for the composition plots of figures 5.4a and 5.4b are given in figure 5.7.

Some major peaks are noted after 2 minutes ageing at e.g. $\beta=2.5\times10^{+8}\,m^{-1}$ and $\beta=2.0\times10^{+8}\,m^{-1}$. However, in contrast to the behaviour of transforms from binary nickel-aluminium data, no wavelength was persistently present either growing or decaying with continued ageing.

Particle size changes with ageing time, estimated from IAP images and QAP traces, were consistent with the $t^{1/3}$ coarsening law, at least after 5 minutes ageing. Data for shorter ageing times showed no definite trends. For all ageing periods a large scatter in particle sizes was found. These results were consistent with the suggestion from TEM that two particle size distributions were present (see

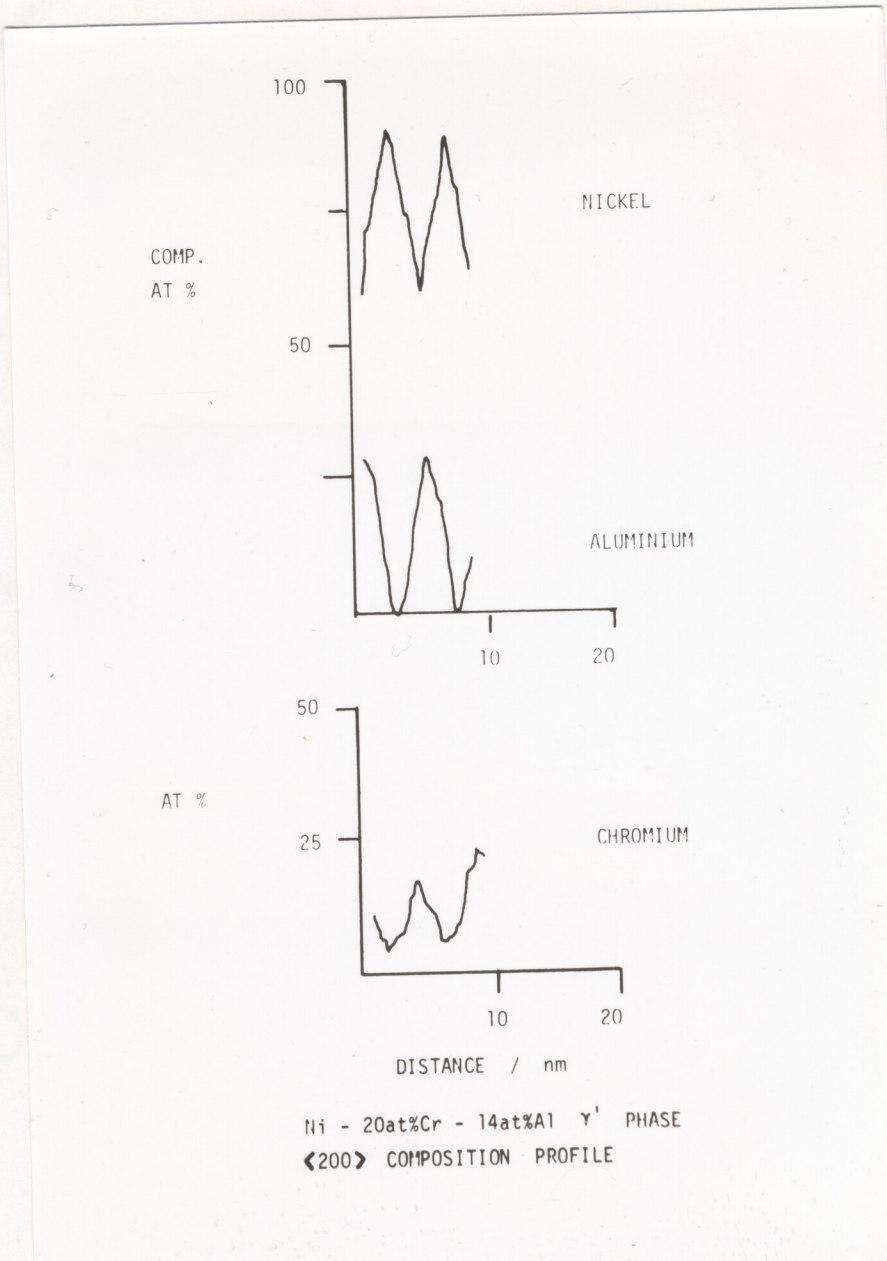
100
NICKEL
COMP.
AT %
50
ALUMINIUM
10
20
50
AT %
25
CHROMIUM
10
20
DISTANCE / nm
Ni - 20at%Cr - 14at%Al γ' PHASE
⟨200⟩ COMPOSITION PROFILE

Figure 5.8

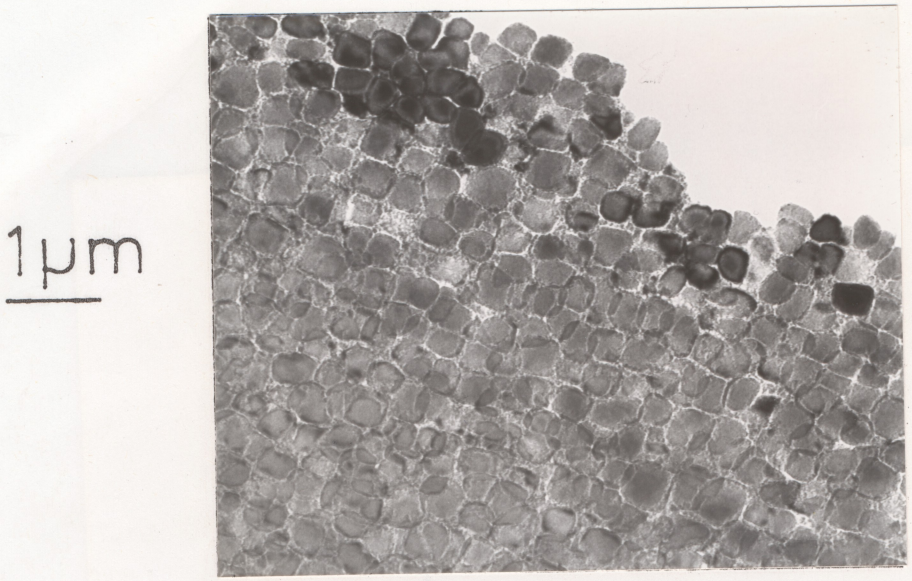

Figure 5.9 Transmission electron micrograph of Ni-20.0at.%Cr-14.0at.%Al alloy as quenched.

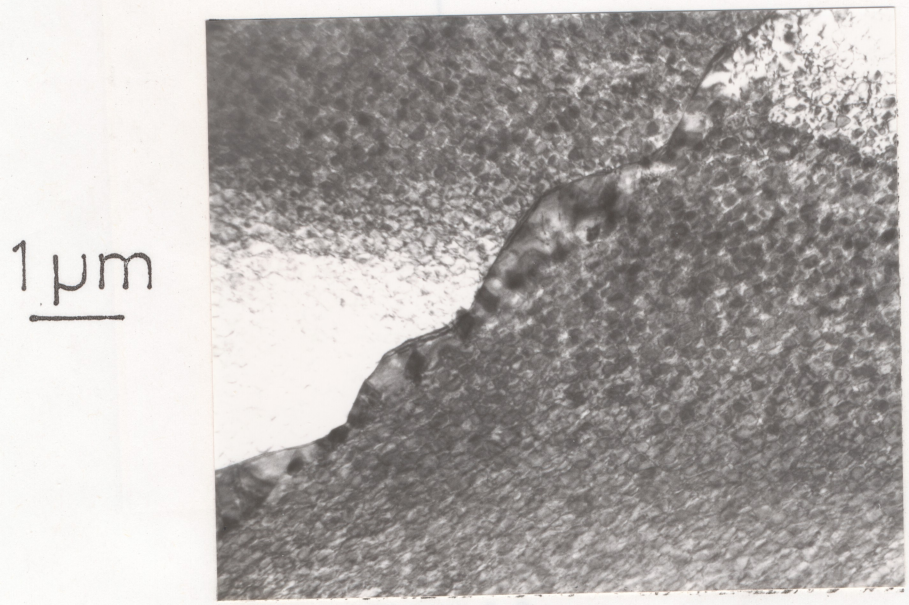

Figure 5.10 Cellular colonies at a grain-boundary in the as-quenched material.

section 5.2.II.2 below).

5.2.II.1iv Quantitative studies III : compositional fluctuations in ordered phase

Figure 5.8 shows a short QAP analysis taken along <100> in an ordered aluminium-rich particle after 5 minutes ageing. The data give composition as a running mean (average over 200 ions, steps of 10) against ion count. Significant compositional modulations are present with the nickel and aluminium traces apparently moving in exact antiphase. The chromium count lags behind both the aluminium and nickel traces, but shows the same periodicity of approximately 460 ions (see section 5.2.III.1ii below).

Maxima and minima for the aluminium are approximately 30at.% and 0at.%. Corresponding minima and maxima for nickel are 60at.% and 90at.%. The overall particle composition was Ni-15.2at.%Al-9.7at%Cr.

5.2.II.2 Transmission Electron Microscopy

TEM studies confirmed APFIM observations of the intragranular two-phase microstructure at all stages of ageing. The as-quenched state is illustrated in the micrograph of figure 5.9. Copious second phase is present with partly globular/partly cuboidal morphology. Alignment is along <100>. Again a wide variety of particle sizes is seen. In some regions of the material larger particles are interspersed with precipitation on a much finer scale. The latter appeared to be modulated (wavelength ~8nm). Cuboidal morphology developed in the second phase with ageing.

Cellular precipitation was found in grain boundary regions of

material, even in the as-quenched alloy (Figure 5.10).

Selected area diffraction patterns were also studied carefully to ascertain the number of phases present. In all cases reflections of f.c.c. matrix and primitive $L1_2$ superlattice phase were found, but no orthorhombic (i.e. Ni_2Cr) reflections were detected.

5.2.II.3 X-ray Powder Diffraction

X-ray powder patterns showed strong reflections of f.c.c. character (3,4,8 etc.) and weaker lines corresponding to the intermediate primitive ($L1_2$) positions (1,2,5 etc.). Some additional reflections also occurred at small Bragg angles, but these did not correspond to expected orthorhombic data.

Some sidebands were found for specimens aged 2-20 minutes. Corresponding modulation wavelengths (Daniel and Lipson 1943) were in the range 9.0-13.0nm. At the high Bragg angle positions reflections became increasingly diffuse with continued ageing.

5.2.III Discussion

5.2.III.1 Atom Probe Data

5.2.III.1i General Microstructure

Throughout the ageing sequence APFIM revealed a two-phase microstructure comprising discrete particles of a major aluminium-rich phase embedded within a chromium-rich phase.

Overall chemical analyses in the range (Ni-20.0at.%Cr-14.0at.%Cr)-(Ni-16.7at.%Cr-14.5at.%Al%Cr) indicate that these phases are probably $L1_2$ ordered γ' (major constituent) and

disordered γ (minor phase) (Taylor and Floyd 1952a).

Examined in detail compositions close to Ni-16.7at.%Cr-14.5at.%Al must be very near to the γ' phase field at 620°C. This would result in a much higher volume fraction of γ' than that observed. Therefore, and in agreement with APFIM analyses, the net composition must be approximated as Ni-20.0at.%Cr-14.0at.%Al. The deviation from the designed zero-mismatch composition (Ni-15.5at.%Cr-14.0at.%Al, Davies and Johnston 1970) may be expected to result in small γ / γ' lattice disregistry. Certainly the microstructure shows two characteristics which are associated with such mismatch (Chapter 1): i) alignment of δ' phase along <100>, and ii) a change from globular to cuboidal morphology with ageing, e.g. Gleiter and Hornbogen 1967a). Using data from Davies and Johnston 1970 the mismatch for Ni-14at.%Al-20at.%Cr was estimated as ~0.20-0.25%.

5.2.III.1ii QAP Analysis

Even before full analysis of QAP traces it was noted that for at least one heat treatment (5 minutes) more than one population of precipitate compositions existed. Similar observations were made for the matrix. In any series of atom probe experiments there is a danger that a misleading variety of particle compositions may be achieved. By indiscriminate simultaneous sampling of both γ and γ' phases compositions ranging from pure γ to pure γ' may be found. However, in present analyses particular care was taken to reject any interface measurements. Furthermore, comparison of the γ' compositions (Ni-17at.%Al-9at.%Cr) and (Ni-26at.% Al-11at.%Cr) showed that a move to lower aluminium content was accompanied by an increase in nickel

but a decrease in chromium. In a material where nickel and chromium partition to the same phase (γ)the compositional variation cannot be explained by partial sampling of γ. The observed changes were greater than the possible error in compositional analyses: it was therefore concluded that there were two γ' populations for the 5 minute heat treatment.

With respect to the origin of the two populations, specimen inhomogeneity was considered unlikely as observations of each case were not confined to a single specimen. It is likely, however, that the effect could be associated with primary precipitation during the quench and later secondary γ' formation (perhaps dependent upon the presence of heterogeneous nucleation sites). This could also give rise to two size distributions. Certainly a wide variety of particle sizes was seen and some TEM images suggested two particle distributions.

Such duplex structure has been observed for other nickel-chromium-aluminium alloys by Beardmore 1969. In the present case and in many others the morphology and distribution of the fine-scale γ' resembles microstructures which are known to result from spinodal decomposition (see section 1.4.3). Certainly, as stated in chapter 1 above, microstructure cannot provide a reliable guide to mechanisms of phase separation, but these results raise the possibilty that secondary γ' may be produced spinodally in these alloys. This effect remains to be investigated in detail for the present alloy.

The two specific compositions for the γ' phase were Ni-17at.%Al-9at.%Cr and Ni-26at%Al-11at.%Cr. If nickel and aluminiun were to occupy only the lattice sites appropriate to a fully ordered

$L1_2$ structure it is possible that the two situations represent $Ni_3(Al,Cr)$ and $(Ni,Cr)_3Al$ structures.

Composition modulations detected by APFIM in Ni-17at.%Al-9at.%Cr have been shown in figure 5.8. It appears that the nickel:aluminium ratios on alternate atomic planes (230 ions per plane) are approximately 100:0 and 50:50. These are the correct ratios for {200} planes in $L1_2$ structures, with aluminium occupying "correct" sites. The remaining element, chromium, appears to be partitioned between the two sets of planes. This suggests a structure $(Ni,Cr)_3(Al,Cr)$. However, it should be noted that, contrary to simplifying assumptions of random evaporation events, some species may be preferentially retained or evaporated from alloys. Thus the exact disposition of elements cannot be determined, although it may appear that the phase is $(Ni,Cr)_3(Al,Cr)$.

Greater detail concerning ordering and compositional modulations in this phase and Ni-26at.%Al-11at.%Cr may possibly be determined using plane stability ratio measurements (e.g. Sinclair, Ralph and Leake 1973).

For heat treatments other than 5 minutes QAP analysis indicated a single γ population of approximately constant composition.

5.2.III.1iii Phase changes

No transformation mechanism could be assigned to γ' generation on the basis of APFIM data. There was no evidence of an incubation time (conventional nucleation) or of increasing compositional modulation (continuous phase separation). Morphological observations suggested that secondary γ' might be produced by spinodal phase separation.

Fourier analyses of QAP traces reflected periodicity of the modulated structure, but showed no persistently dominant wavelengths which might indicate spinodal change (e.g. Cahn 1968; de Fontaine 1979; also Chapter 4).

It is possible, however, that further data concerning the possibility of spinodal change may be obtained by more detailed studies of particle size as a function of ageing time for ageing periods less than 5 minutes i.e. before $t^{1/3}$ coarsening is established. Present data show no definite trends in particle size at these times and the possibility of a constant size plateau corresponding to constant wavelength continuous change (Sinclair, Leake and Ralph 1974) should be examined.

5.2.III.2 TEM and X-ray analyses

These subsidiary results confirmed APFIM studies of the modulated γ/γ' microstructure. In particular both techniques recorded $L1_2$ lattice reflections from the ordered phase.

The separate lattice parameters of the two phases could not be resolved with any certainty in the X-ray powder patterns (0.001nm is the resolution of standard cameras). However, the small degree of strain in the structure was observed to broaden high angle lines with ageing : size broadening should decrease as the structure coarsens.

No reflections from ordered orthorhombic Ni_2Cr-type phase were found in material after any quench. Even in pure Ni_2Cr phase a high degree of long range order appears only after a prolonged anneal, and below 590°C (Vintaykin and Urushadze 1969). However, it should be noted that the matrix contains approximately 34at.% chromium and Pt_2Mo

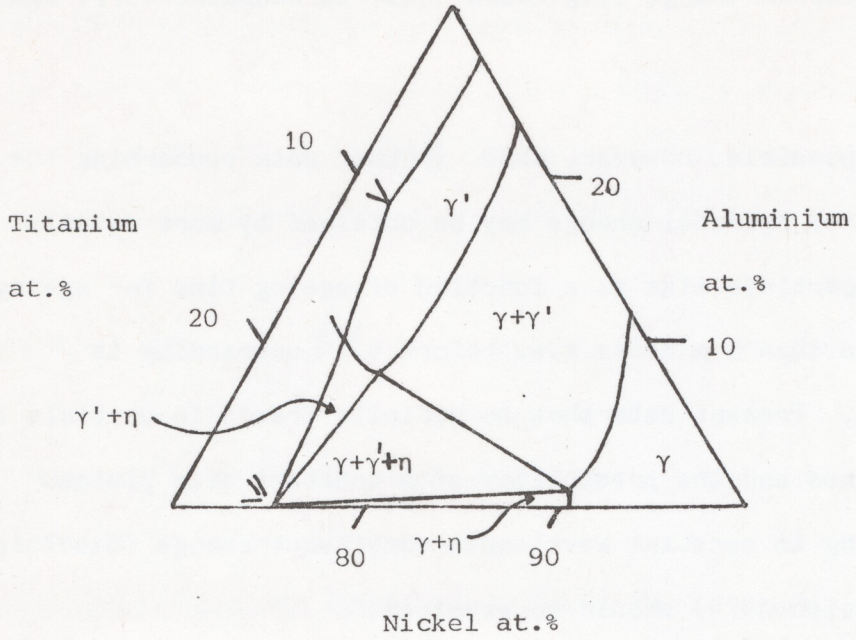

Figure 5.11 The nickel-aluminium-titanium phase diagram: isothermal section for 750°C (after Taylor and Floyd 1952a).

structure formation should be borne in mind for long heat treatment at lower temperatures.

Cellular precipitation at grain boundaries was consistent with data of Hornbogen and Roth 1967.

5.3 Nickel-Titanium-Aluminium

5.3.I Phase Relationships

A section of the equilibrium phase diagram for nickel-aluminium-titanium at 750°C, taken from Taylor and Floyd 1952a, is shown in figure 5.11. The γ and γ' (Ni_3Al) phases of the nickel-aluminium system have already been discussed in Chapter 4. On the nickel-titanium side the equilibrium components are γ matrix and hexagonal η Ni_3Ti (Taylor and Floyd 1952a; Hansen and Anderko 1958), thus restricting γ' to aluminium-rich $Ni_3(Al,Ti)$ compositions. Taylor and Floyd 1952a originally measured the extent of substitution by titanium for aluminium as 60%.

However, under non-equilibrium conditions Ni_3Ti may precipitate first as metastable γ' ($L1_2$) phase, isostructural with Ni_3Al (e.g. Bagariatskii and Tyapkin 1957; Buckle, Gentry and Manenc 1959; Mihalisin and Decker 1960). Mixed, ordered $Ni_3(Al,Ti)$ phase of any Al/Ti ratio is therefore possible in the ternary system, under similar non-equilibrium conditions(Mihalisin and Decker 1960). As with the component binary systems, lattice mismatch between precipitate and matrix gives rise to modulated two-phase γ/γ' microstructures, with γ' in cubic or globular form. In the binary end-products separation of the new phase may occur by either nucleation-plus-growth or continuous processes, the former at low supersaturations and the

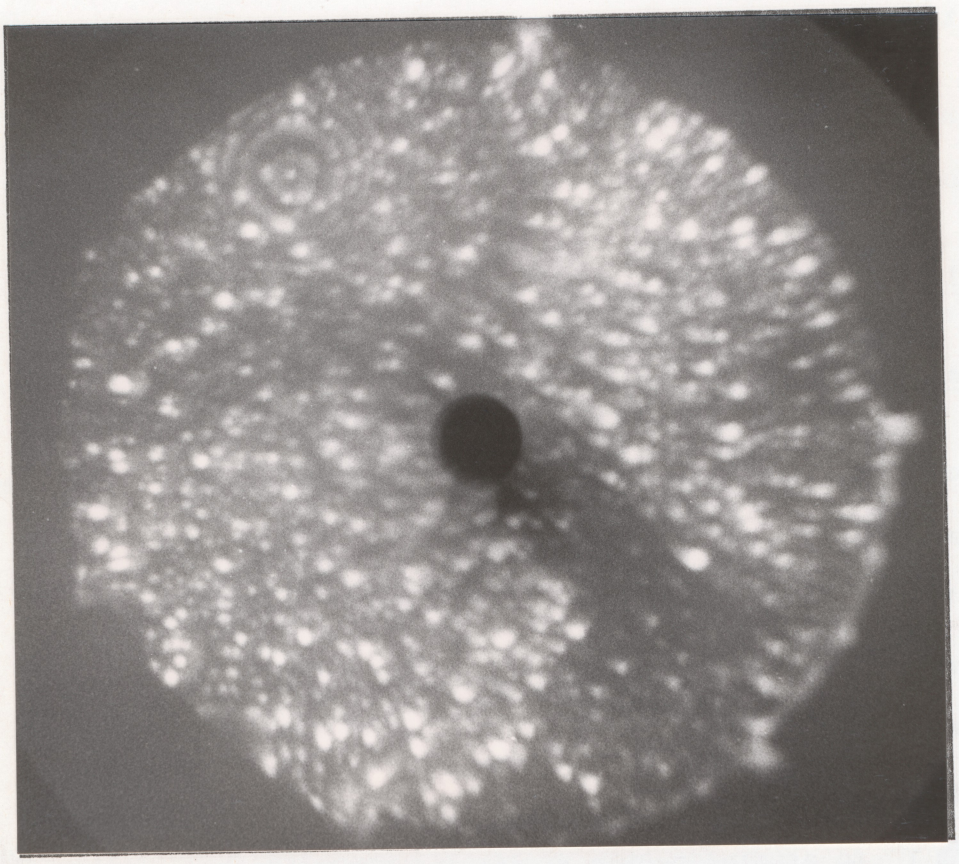

Figure 5.12a Field-ion micrograph of Ni-9.1at.%Al-4.4at.%Ti alloy quenched from 1250^{o}C.

b) c)

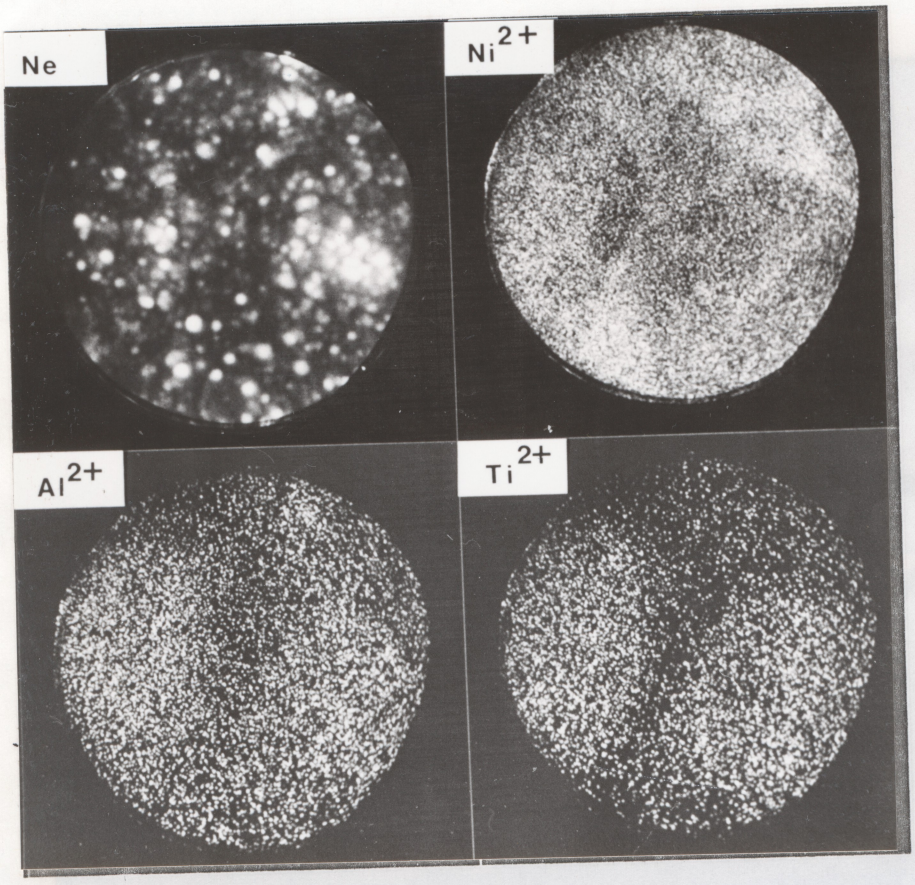

d) e)

Figure 5.12b-e IAP images from alloy quenched from 1350°C - b) FIM image, c) Ni^{2+}, d) Al^{2+}, e) Ti^{2+}.

latter at high supersaturations (for nickel-aluminium see Chapter 4, for nickel-titanium (e.g. Sass and Cohen 1969 (nucleated); Sinclair, Leake and Ralph 1974; Laughlin 1976; Watts and Ralph 1977 (continuous)). Phase transformations in the ternary alloys have not been pursued, however.

More interest has been shown in the use of the system to model the role of coherency strains in the hardening of superalloys (e.g. Fine 1968; Phillips 1968; Decker and Mihalisin 1969; Parker 1970). These workers found some effect of coherency in the observed hardening by titanium (Guard and Westbrook 1959, Mihalisin and Decker 1960) but concluded that other mechanisms were also operative (see Chapter 1).

5.3.II Results

5.3.II.1 Alloy 1: Ni-9.1at.%Al-4.4at.%Ti

5.3.II.1i Quenched alloy

All quenched specimens exhibited γ' precipitation with particle sizes in the range 20-30nm whether homogenised and quenched from 1350°C, 1250°C or 1050°C. FIM observation suggested that precipitates were smaller and more numerous in the 1350°C pre-quench specimens, but quantitative analysis was not performed. The particles presented well-defined cuboidal morphology and in many cases appeared to be ogdoadically diced. These features are illustrated by figure 5.12a which shows a field-ion image of material quenched from 1250°C. The micrograph was taken at 6.6 kV, just below best imaging voltage, in order to accentuate the protruding precipitates. Some degree of order may be observed within the particles. No evidence of nucleation upon dislocations was seen. Figures 5.12b-e show the preferential

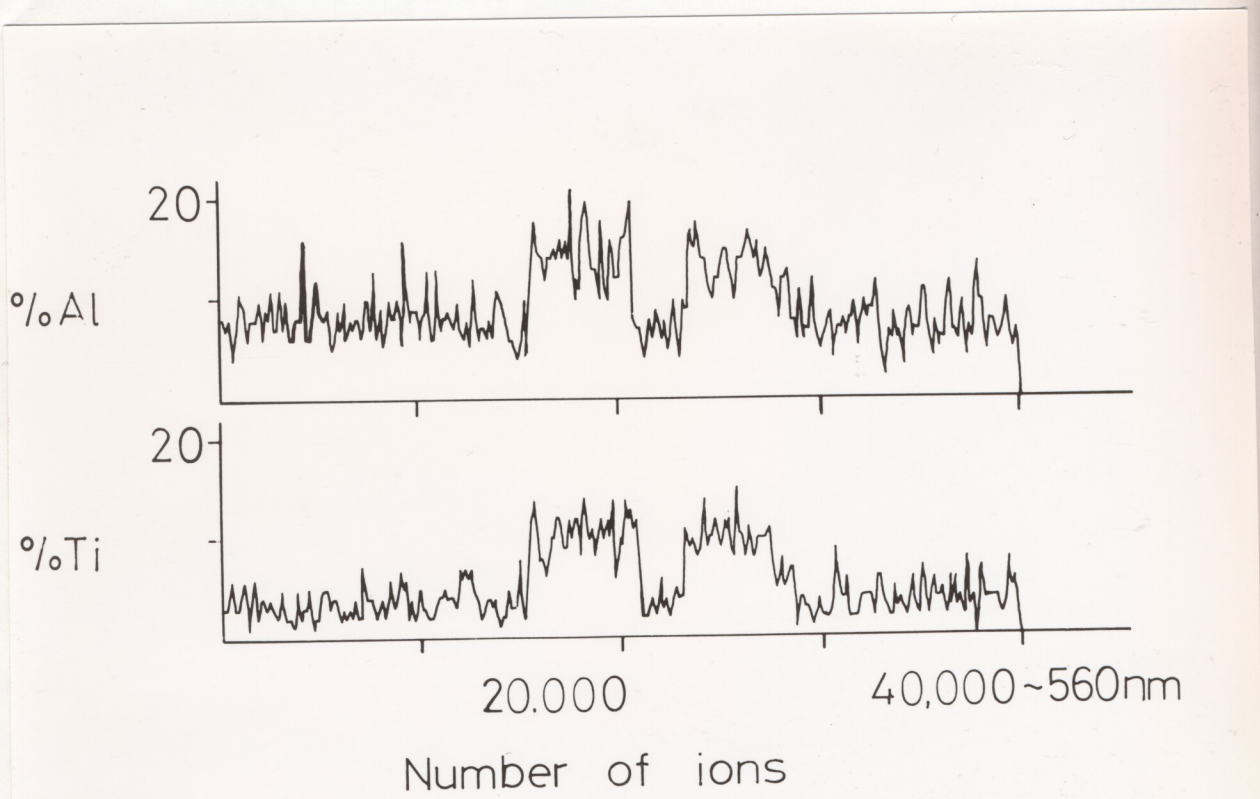

Figure 5.13 Profiles of aluminium and titanium contents against distance for the specimen of figure 5.12a (<110> probing direction).

Table 5.3. QAP Analyses of Ni-9.1at%Al-4.4at%Ti: γ' Phase

Heat Treatment	Al/at%	Ti/at%	Ni/at%
Homogenised @ 1050°C, quenched	16.05 ±1.43	8.28 ±1.03	75.67 ±3.11
Homogenised @ 1250°C, quenched	14.06 ±0.20	10.19 ±0.17	75.75 ±0.45
Homogenised @ 1350°C, quenched	11.76 ±0.34	9.30 ±0.30	78.95 ±0.87
Homogenised @ 1350°C, quenched, aged for 1 hour at 625°C	13.24 ±0.46	8.97 ±0.38	77.78 ±1.11
Homogenised @ 1350°C, quenched, aged for 5 hours @ 625°C	12.13 ±0.19	10.25 ±0.18	77.62 ±0.49

Table 5.4 QAP Analyses of Ni-9.1at%Al-4.4at%Ti: Matrix Phase

Heat treatment	Al/at%	Ti/at%	Ni/at%
Homogenised @ 1050°C, quenched	8.76 ±0.22	4.45 ±0.16	86.78 ±0.70
Homogenised @ 1250°C, quenched	7.93 ±0.13	3.91 ±0.09	88.16 ±0.43
Homogenised @ 1350°C, quenched	7.51 ±0.10	4.12 ±0.07	88.38 ±0.32
Homogenised @ 1350°C, quenched, aged for 5 hours @ 625°C	5.18 ±0.10	3.26 ±0.08	91.56 ±0.43

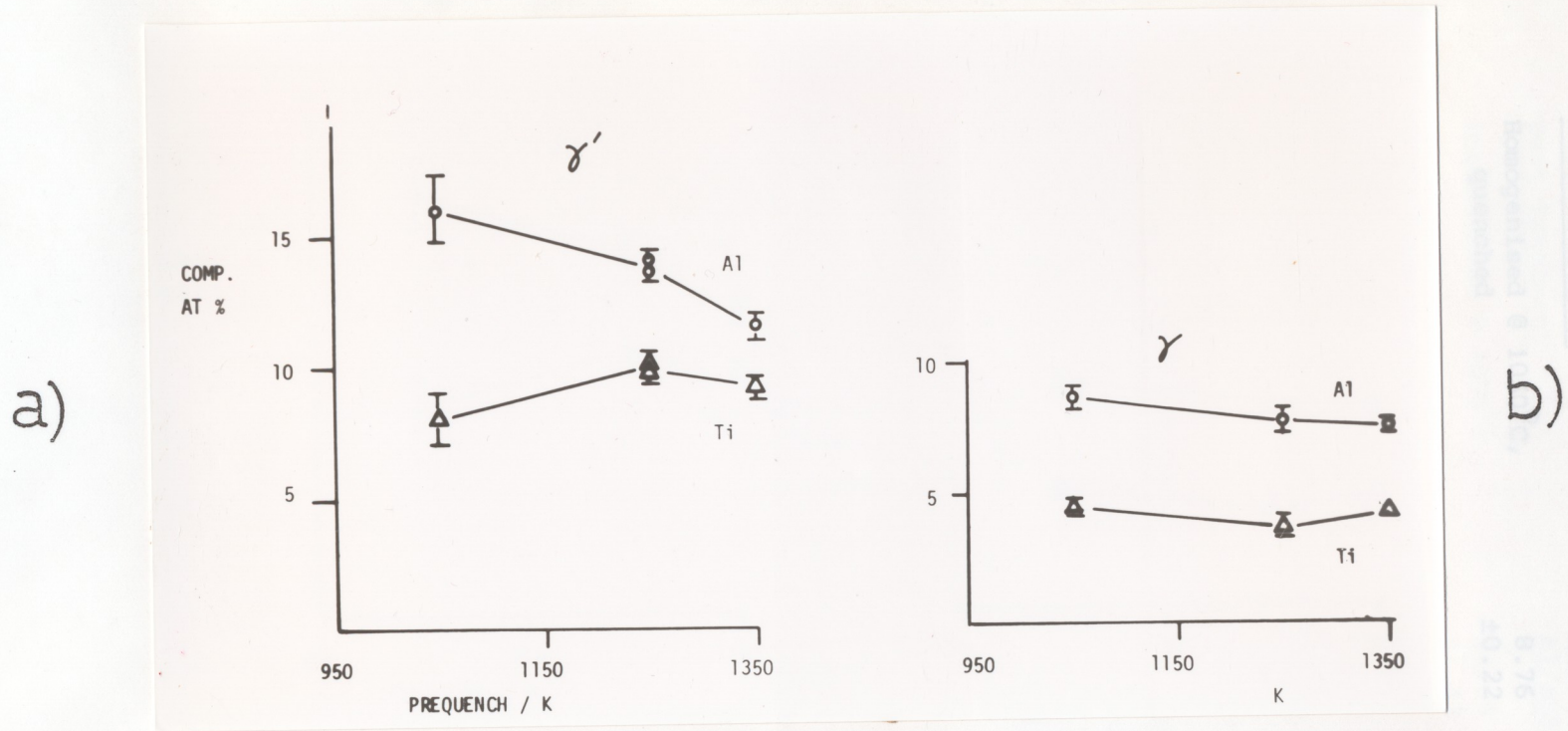

Figure 5.14 Ni-9.1at.%Al-4.4at.%Ti:- compositions of a) precipitate and b) matrix, as a function of prequench temperature.

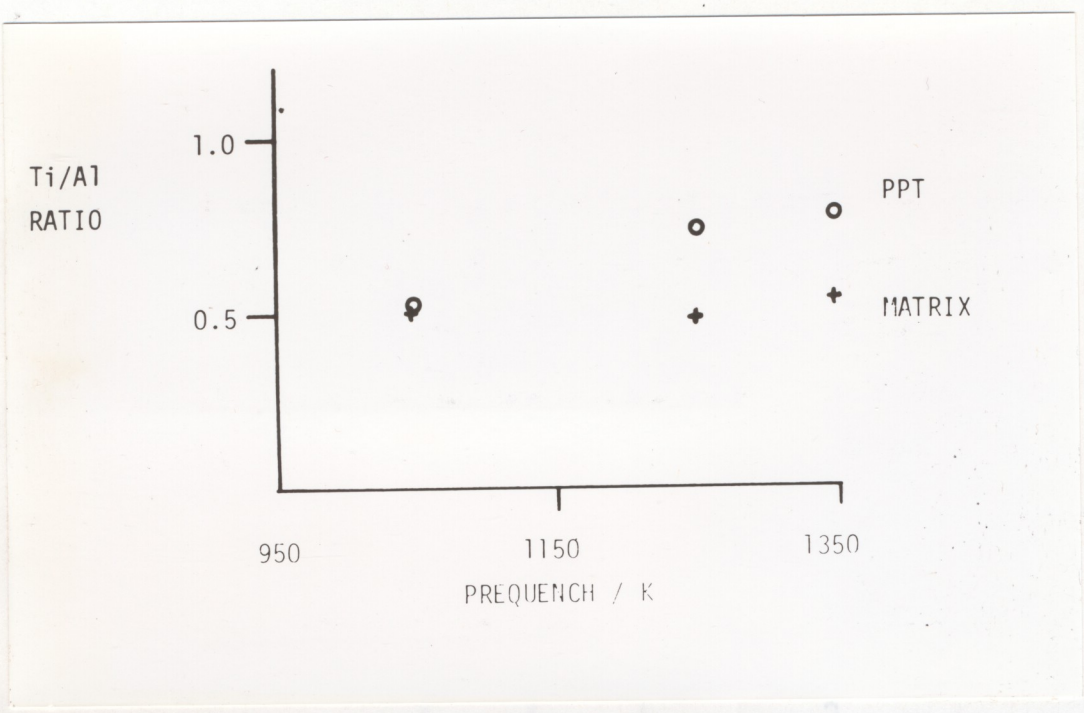

Figure 5.15 Ni-9.1at.%Al-4.4at.%Ti. Ratio of Ti to Al in γ' phase as a function of prequench temperature.

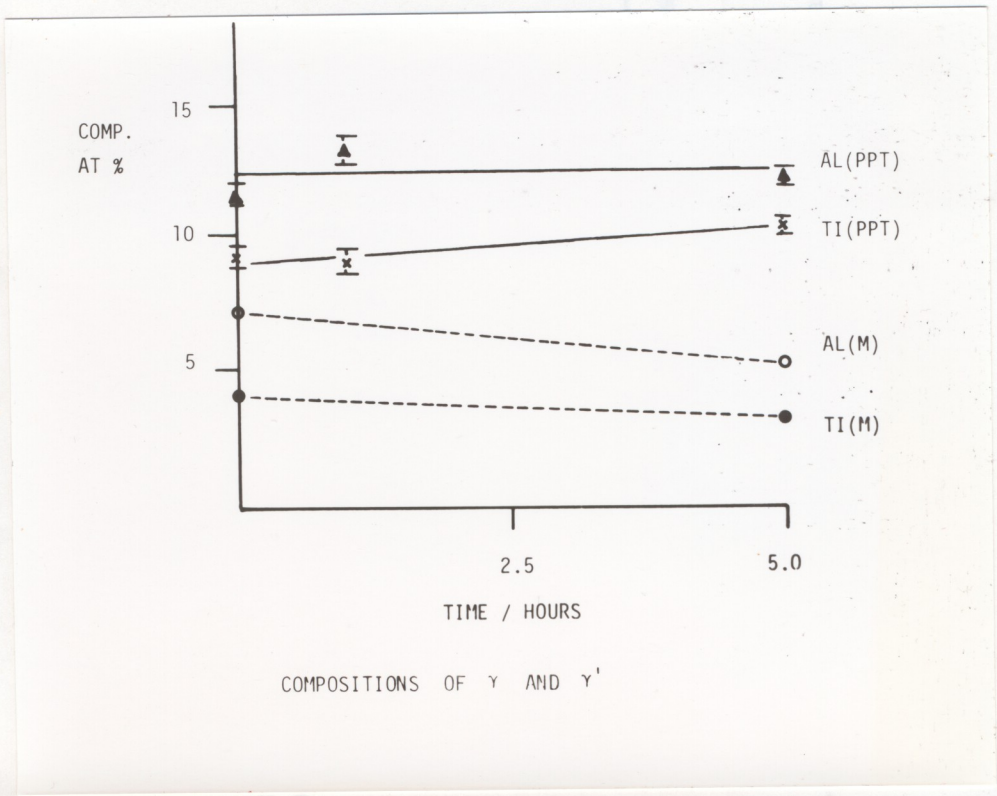

Figure 5.16 Ni-9.1at.%Al-4.4at.%Ti. Compositions of the two phases as a function of ageing time for a prequench temperature of 1350°C.

partitioning of aluminium and titanium to the γ' phase.

Figure 5.13 presents APFIM traces of aluminium and titanium contents versus probing distance taken from the specimen illustrated in figure 5.12a.The probing direction was <220>. Two well-defined γ' particles, of total (Al+Ti) content approximately 25at.%, are visible. Compositions in the γ matrix oscillate about a total mean of approximately 11.5at.%.

Precipitate and matrix regions of APFIM traces from the three types of quenched specimens were analysed quantitatively to assess the effect of the quench. The results are shown in figures 5.14a and 5.14b. Figure a) gives the aluminium and titanium contents in the precipitate as a function of the temperature from which quench took place. Figure b) presents similar data for the matrix. Two effects may be noted in the precipitate region. Firstly, as the pre-quench temperature is raised the total (Al+Ti) content of the second phase decreases from approximately 25at.% (as required for stoichiometry) to about 21at.%. Secondly, the ratio of Ti to Al becomes significantly enriched from ~0.5(±0.05) to ~0.8(±0.05) (figure 5.15). This occurs mainly by decrease in aluminium content but with a slight increase in titanium. The matrix composition remains approximately constant throughout the temperature range, although a slight downward trend in aluminium content may be noted with increasing temperature. (Tables 5.3 and 5.4).

5.3.II.1ii Heat-treated alloy

Partitioning was also studied as a function of ageing time at 625°C for alloys quenched from 1350°C. The results of QAP analysis of precipitates are shown in figure 5.16. Both aluminium and titanium contents increase slowly with time. A slight enrichment of the titanium/aluminium ratio is seen as the titanium content increases

Figure 5.17 Paired dislocations in quenched Ni-8.7at.%Al-2.5at.%Ti.

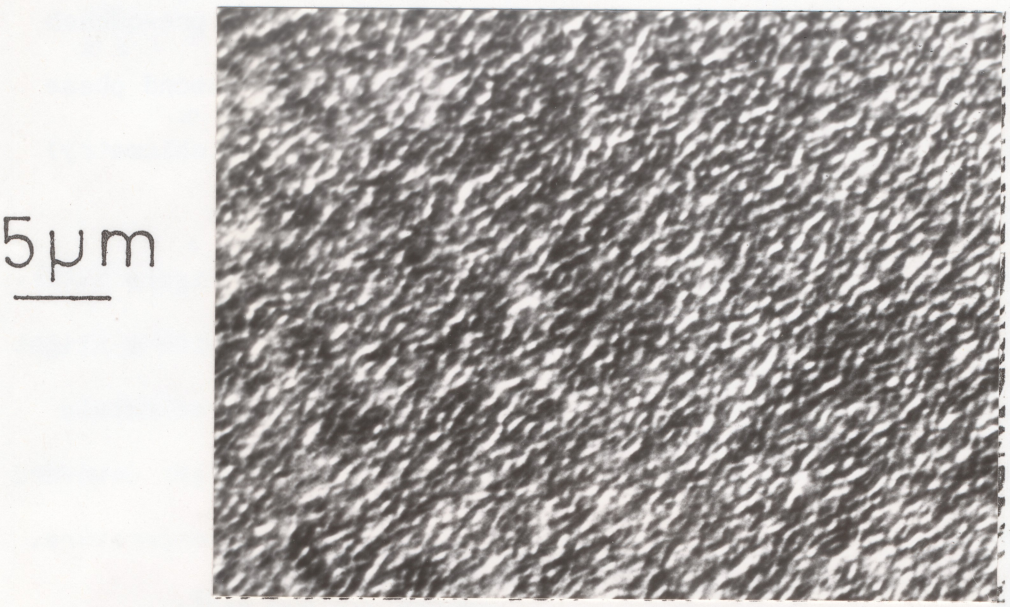

Figure 5.18 Mottled contrast in Ni-8.7at.%Al-2.5at.%Ti alloy aged for 5 hours at 625°C.

slightly more rapidly than that of aluminium. It should be noted the the overall (Al+Ti) content rises towards stoichiometric ($Ni_3(Al,Ti)$), increasing from ~21at.% to ~23.5at.% with five hours heat treatment. Corresponding decreases in aluminium and titanium contents of the matrix were seen: the aluminium content dropped from 7.5 to 5.2at.% and titanium from 4.1 to 3.3at.% (errors are ± 0.10 at.%). These changes were accompanied by particle coarsening from 20-30nm mean diameter to 30-40nm.

5.3.II.2 Alloy 2: Ni-8.7at.%Al-2.5at.%Ti

Similar precipitation was observed in quenched and heat-treated Ni-8.7at.%Al-2.5at.%Ti alloy, with superlattice reflections from ordered γ' particles present in all SADP. Sets of paired dislocations were observed in quenched material (figure 5.17). No mottled bright field contrast was seen in quenched alloy, but some "tweed"-type effects were visible after five hours of ageing. This is shown in figure 5.18. No evidence of η phase was observed.

5.3.III Discussion

5.3.III.1 General Precipitation

The presence of copious precipitation with square waveform composition profiles upon quenching both alloys may suggest phase separation by nucleation. This is in contrast to the behaviour of Ni-14.1at.%Al alloy. However, small changes have been effected in the lattice mismatch (Ni-14.1at.%Al alloy +0.56%, nickel-aluminium-titanium alloys >+0.6%, Taylor and Floyd 1952a). In addition a slightly lower volume fraction of γ' phase is present. Given also that the original binary alloy must itself lie relatively close to the

incoherent miscibility gap, by virtue of its composition, it would seem reasonable that minor changes in strain and chemical gradient terms could favour conventional nucleation mechanisms.

The observations of aligned microstructures are consistent with a large misfit parameter (see also e.g. Mihalisin and Decker 1960).

The presence of superlattice reflections in diffraction studies and ordered planes in APFIM micrographs suggest that ordering in occurs early in phase separation. The dislocation pairs of figure 5.17 are characteristic of γ/γ' microstructures containing ordered $L1_2$ phase (e.g. Gleiter and Hornbogen 1965a, 1965b).

Additional observations of "tweed"-like contrast after ageing may be attributed to an increasing degree of order in the microstructure and growth of ordered domains.

5.3.III.2 Compositional Changes and Precipitation Mechanisms

Materials of high precipitate/matrix lattice mismatch often nucleate heterogeneously. No evidence of nucleation on dislocations was observed in the present study. Other possible catalytic sites are vacancies and solute atoms. The effect of vacancies may be examined by changing the pre-quench temperature - as this temperature is raised the equilibrium concentration of vacancies also increases.

Observations of precipitate number densities and sizes suggested that fewer but larger particles were present in material quenched from lower temperatures. This would imply that nucleation is vacancy catalysed. The result remains to be confirmed by accurate number density counts.

The effect of pre-quench upon composition of γ' was investigated, however. QAP analysis demonstrates first of all that non-stoichiometric low alloy content γ' may be generated. This is to be expected where the phase field shows a wide range of compositions. Analysis of quenched and aged alloy for 1350°C pre-quench shows further that the titanium-aluminium ratio changes upon ageing, and that the sum total of the two elements increases towards 25at.%. That the total alloy content changes suggests initial nucleation, by heterogenous or catalytic means, of a non-equilibrium phase. Adjustment of the titanium/aluminium ratio alone, in these or other alloys, may be a function of ordering atom exchange.

As the pre-quench temperature is lowered the total (Al+Ti) content approaches 25at.% and the Ti/Al ratio decreases to 0.5 in the precipitate. These data suggest a major role for vacancies in γ' formation. With respect to initial γ' composition it is possible that the Ti/Al ratio is determined by the vacancy assisted diffusion of the two elements, with aluminium diffusing the faster. It would appear that the total (Al+Ti) content, however, is a function also of vacancy concentration. This may imply that, as the total vacancy concentration is raised, a greater proportion of vacancies act as nucleation sites rather than diffusing species, and the net γ' composition is partly kinetically controlled.

It should also be noted that general trends in precipitate composition with pre-quench temperature and ageing time were approximately mirrored by opposite changes in matrix composition. A small overall loss in aluminium and titanium content which was noted as the pre-quench temperature was raised may be associated with

elemental loss by evaporation from the specimen surface . Thus changes in overall composition should not affect the general conclusions.

5.4 Summary

5.4.1 Nickel-Chromium-Aluminium Alloy

A two-phase microstructure of $L1_2$ ordered γ' and disordered f.c.c. γ phases was observed at all stages of ageing at 620°C. The γ' phase was partially aligned along <100> and changed from globular to cuboidal morphology with ageing. This was consistent with an estimated γ/γ' lattice mis-match of ~0.20-0.25%. The mean phase compositions were approximately constant overall at Ni-20.5at.% Al-9.5at.%Cr(γ') and Ni-34.0at.%Cr-6.5at.%Al(γ). Two populations of each of the γ' and γ phases were noted for the 5 minute heat treatment. The possible origins of these structures were discussed although no transition mechanisms could be identified for γ' generation. No evidence of an orthorhombic structure was found.

Cellular precipitation was noted at grain boundaries and coarsening data were in accord with previous observations.

5.4.2 Nickel-Titanium-Aluminium alloys

Precipitation of ordered γ' phase was observed in both Ni-9.1at.%Al-4.4at.%Ti and Ni-8.7at.%Al-2.5at.%Ti upon quenching. It was shown that the initial composition of the second phase depends upon pre-quenching temperature: Ni-9.1at.%Al-4.4at.%Ti shows a total (Al+Ti) content of ~25at.% upon quenching from 1050°C, with a Ti/Al ratio of 0.5 ± 0.05. Quenched from 1350°C the alloy content is

~21at.%, and the Ti/Al ratio is 0.8 ±0.05. Ageing of alloy quenched from 1350°C promoted an increase in (Al+Ti) content. It was suggested that the second phase is generated by heterogeneous nucleation, and the role of vacancies in nucleation and control of second phase composition was discussed.